DOI: 10.53704/fujnas.v13i2.545

A publication of College of Natural and Applied Sciences, Fountain University, Osogbo, Nigeria.
Journal homepage: www.fountainjournals.com
ISSN: 2354-337X(Online),2350-1863(Print)

# Green Synthesis of Copper Oxide Nanoparticles for Improved Performance in Monolithic Dye-Sensitized Solar Cells

**[1,2]Abiodun, A. J., [1]Alamu, G. A., [2]Daramola, O. O., [1,3*]Adedokun, O., [1,3]Sanusi, Y. K.**

[1] *Department of Pure and Applied Physics, Ladoke Akintola University of Technology, P.M.B. 4000, Ogbomoso, Nigeria*
[2] *Department of Physics, Lead City University Ibadan, Oyo Nigeria*
[3]*Nanotechnology Research Group (NANO+), Ladoke Akintola University of Technology, Ogbomoso, Nigeria.*

## Abstract

This research investigated the impact of incorporating green synthesised copper oxide nanoparticles into nanoporous carbon counter electrodes to enhance photovoltaic performance in Monolithic Dye-Sensitized Solar Cells (MDSSCs). Copper oxide nanoparticles were successfully synthesised using an extract from *Ocimum gratissimum* leaves. Optical absorption between 250 nm and 400 nm confirmed the formation of copper oxide nanoparticles. XRD patterns indicated the crystalline nature of the copper oxide nanoparticles, with an average crystallite size of 47.9 nm. FTIR analyses identified chemical bonds potentially responsible for nanoparticle formation**.** MDSSC performance evaluation demonstrated a significant 3.5% increase in efficiency over the cells without nanoparticles, this translates to a 105.9% increase in efficiency observed for cells with the nanoparticles. The incorporation of green-synthesized copper oxide nanoparticles into the counter electrode of MDSSCs exhibited an eco-benign and even dispersion, suggesting its potential as a promising nanomaterial for DSSC applications.

**Keywords:** Green Synthesis; Nanoparticles; Copper Oxide; Counter Electrode; Monolithic Dye -Sensitised Solar Cell

## Introduction

Dye-sensitised solar cells (DSSCs) have emerged as an economically viable option for nanostructured solar cells. Traditionally, DSSCs consist of a layered configuration comprising a counter electrode and a mesoporous oxide structure acting as a photoanode with a thermo-plastic polymer serving as a spacer layer in between. The space between the electrodes is filled with an electrolyte containing redox ions, typically $I^-/I^{3-}$ ions. Photoelectrons are generated via photon absorption and transferred from the highest occupied molecular orbitals to the lowest unoccupied molecular orbitals of the dye molecules. These electrons then enter the electron-conducting nanostructures, typically $TiO_2$, and flow through the external circuit. The $I^-$ ions facilitate the reduction of the dye molecules, with diffused $I^{3-}$ ions subsequently being reduced to $I^-$ ions on the counter electrode surface (Aghazada *et al.,* 2016; Higashino *et al.,* 2015; Huang *et al.,* 2016; Li *et al.,* 2016; Liang *et al.,* 2013; Wild *et al.,* 2016). Extensive research has explored various aspects

*Corresponding Author: https://orcid.org/0000-0002-7947-8415
Email address: oadedokun@lautech.edu.ng

of DSSC technology, including different dye molecules (Gong *et al.,* 2017; Freitag *et al.,* 2017), catalysts for counter electrodes (Adachi *et al.,* 2013; Ahmad *et al.,* 2014; Ahn *et al.,* 2014; Baker *et al*., 2014; Chen *et al.,* 2017; Yu *et al.,* 2016), diverse metal oxide nano structures such as $TiO_2$ (Lin *et al.,* 2008; Roy *et al.,* 2010; Sharmoukh *et al.,* 2012) and ZnO (Anta *et al.,* 2012; Lin *et al.,* 2011; Lizama-Tzec *et al.,* 2018; Zhu *et al.,* 2014; Zi *et al.,* 2014) nanoparticles, nanorods, and nanotubes, as well as a wide array of electrolytes featuring different redox couples (e.g., Co Yella *et al.,* (2011) and Cu (Freitag *et al*., 2017 & Bai *et al.,* 2011) complexes, $Br^-/Br^{3-}$ (Bella *et al*., 2015), SeCN−/(SeCN)2 (Oskam *et al.,* 2001), and ferrocene derivatives (Bella *et al*., 2015), and solvent variations. Recently, nanocomposite polymer electrolytes have also been found to be applicable in DSSCs (Zebardastan *et al.,* 2017). In terms of DSSC manufacture, a great deal of research has been done on the photoanode. $TiO_2$-based photoanodes are among the most effective; however, they only absorb ultraviolet (UV) radiation, which is a very small percentage of the solar spectrum. As a result, dye molecules absorb visible light by acting as sensitizers (Gratzel, 2005). Although ruthenium-based dyes have a strong visual absorption as sensitizers, their expensive manufacturing and undesirable environmental effects have led researchers to explore natural dyes as substitutes (Adedokun *et al.*, 2018). Plant materials offer a free source of pigments, such as carotene and chlorophyll, which act as sensitizers (Adedokun *et al.*, 2018). However, natural colours perform far worse than dyes based on ruthenium, which makes the usage of nanoparticles necessary (Aitken *et al.*, 2006). However, there has been limited exploration of alternative configurations to the conventional sandwich-type structure.

The conventional structure poses challenges for flexible dye-sensitized solar cells (DSSCs), as well as DSSCs with a single flexible electrode, due to the high risk of short-circuiting both electrodes. This results from dissimilar spacing between different parts of the cell. In our study, we propose a novel metal-based monolithic structure with an insulating spacer layer covering the entire electrode surface. This approach mirrors other monolithic structures previously employed in DSSCs using porous carbon (Pettersson *et al.*, 2012; Ito *et al.,* 2012; Rong *et al.*, 2013; Liu *et al.*, 2012). As an alternative to carbon electrodes, various porous layers have been suggested, including carbon composites with conducting polymers (Thompson *et al.,* 2013 & Wang *et al.,* 2011), porous titanium layers (Fu *et al.,* 2010 & 2013), and porous platinum-loaded tin-doped indium oxide layers (Takeda *et al.,* 2009). In the case of carbon-based monolithic structures, a thick graphitic layer is necessary to reduce series resistance in the counter electrode. However, thickening the carbon layer on a large scale results in insufficiently low series resistance, leading to poor fill factors in cells. Monolithic structures with graphite/carbon layer composites have been reported to exhibit a series resistance approximately twice that of a fluorine-doped tin oxide (FTO) substrate (Kwon *et al.,* 2013). The issue of mechanical stability does not arise with metal layers. As an alternative to carbon layers, a porous carbon layer deposited through sputtering has been proposed (Wang *et al.,* 2011). However, a drawback of porous carbon layers is that they cannot be thick enough to reduce series resistance effectively. Achieving precise control over the pore size on a large scale using vacuum deposition methods is challenging and expensive. Additionally, the smoothness of the spacer layer is crucial for the quality and series resistance of the metallic layer (Rong *et al.*, 2013). Qureshi *et al.* (2020) show how to alter both functional electrodes in a plasmonic dye-sensitized solar cell (PDSSC) to create an affordable and effective solar gadget. The power conversion efficiency (PCE) of the $Cu/TiO_2$ nanocomposite-based photoanode was 3.89% with Platinum (Pt) and 2.20% with hybrid $rGO/Fe_3O_4$ counter electrodes (CEs), respectively, in PDSSCs also Nursam *et al.,* (2020) worked on fabrication of a monolithic DSSC module with an active area of 10.32 $cm^2$ that contains three individual cells integrated via series connection. After interconnection, the monolithic DSSC module gave an overall photoconversion efficiency of 0.98%, which was unexpectedly higher than the individual cells. As an alternative to carbon layers, a hybrid porous carbon–copper oxide nanoparticle layer has been proposed (Fu *et al.,* 2013).

To address the issues of low conductivity and fragility associated with carbon electrodes and the porosity problem of metal films in monolithic structures, green synthesized copper oxide nanoparticles incorporated into the porous carbon combination is introduced in this study**.** It is important to note that the potential superiority of green synthesis methods for solar cells lies in their environmental friendliness, energy efficiency, cost-effectiveness, scalability, reproducibility, improved product properties, and alignment with regulatory and market trends towards sustainability. These advantages position green synthesis as a promising approach to advancing solar cell technology while minimizing its environmental footprint and enhancing economic viability. In order to investigate the structural and morphological properties of the copper oxide nanoparticles, the nanoparticles were optimized and characterized. Fabrication costs are also decreased when doped porous carbon is used instead of platinum in large-scale production. We developed an enhanced porous carbon counter-electrode in this work while fabricating the DSSC using the monolithic technique. The integration of CuO nanoparticles with carbon-based materials in solar cells aims to improve properties such as conductivity, charge separation and transport, surface area and interface quality, stability, durability, and optical performance. These enhancements collectively advance solar cell technology, making them more efficient, reliable, and suitable for practical applications in renewable energy systems.

## Materials and Methods

### Materials

*Occimum grattissimum* (scent leaf) leaves were acquired from a farm in the neighbourhood of Moniya, Ibadan Oyo state, Nigeria. The chlorin e6 dye and Flourine-doped Tin Oxide (FTO) conducting substrates (50 × 50 × 1.1 mm, 10 Ω/sq) and Zirconia oxide paste ($ZrO_2$) were acquired from Solaronix S.A. Copper nitrate and Titanium dioxide were acquired from Sigma-Aldrich and used without further purification.

### Green synthesis of copper oxide nanoparticles

The *Occimum grattissimum* leaves were collected freshly, washed with deionized water, air-dried and grounded separately to form a fine powder. 100 g of the dried fine powder was boiled in 500 ml of distilled water in a 1000 ml flask for 30 minutes, and the extract was filtered using Whatman no. 1 filter papers, as shown on plate 1.0.

CuO was synthesized with aqueous leaf extract of *Occimum grattissimum* which served as both a reducing and capping agent. In a typical procedure (Bibi *et al*., 2019), plant extract was added drop wisely to Cupric nitrate solution at a ratio of 1:10. A colour change was observed, and the resultant mixtures were then centrifuged and decanted; the pellet was then rinsed out of the centrifuge tubes using ethanol (this also removes impurities) which was dried with argon gas for 2 minutes to dry out the ethanol before completely drying in the oven. The pellets were found to be bluish, which confirmed the synthesis of copper oxide nanoparticles, as shown in plate 2. The combined action of phenolic compounds, terpenoids, alkaloids, and proteins present in Efinrin leaf facilitates the green synthesis of CuO nanoparticles. These phytochemicals act as both reducing agents, facilitating the reduction of Cu (II) ions to CuO nanoparticles, and as capping agents, stabilizing the nanoparticles and controlling their size and dispersibility in solution (Rajesh et al., 2017; Yardily & Sunitha, 2019). This green synthesis approach is advantageous due to its environmental friendliness and potential applications in various fields, including nanotechnology and renewable energy.

When scent leaf extract (containing phytochemicals like phenolic compounds, terpenoids, alkaloids, and proteins) is used as a reducing agent in the synthesis of CuO nanoparticles from copper nitrate, the following simplified chemical reaction can be proposed:

1. Reduction of Copper Nitrate:

Copper nitrate ($Cu(NO_3)_2$) in aqueous solution reacts with the reducing agents present in the scent leaf extract, leading to the reduction of Cu (II) ions to Cu (I) and further to Cu (0) nanoparticles:

$Cu^{2+} + 2e^- \rightarrow Cu^+$

$Cu^+ + e^- \rightarrow Cu^0$

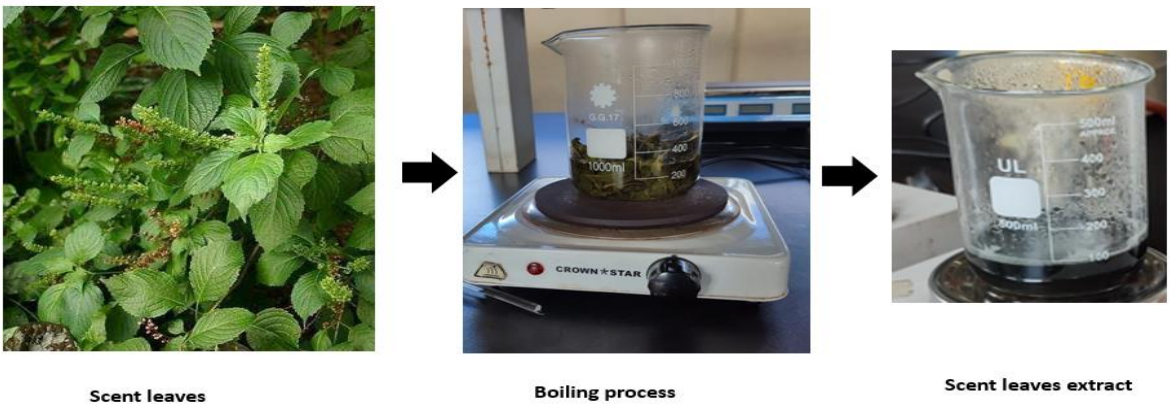


**Plate 1.0: Preparation process of the plant extracts**

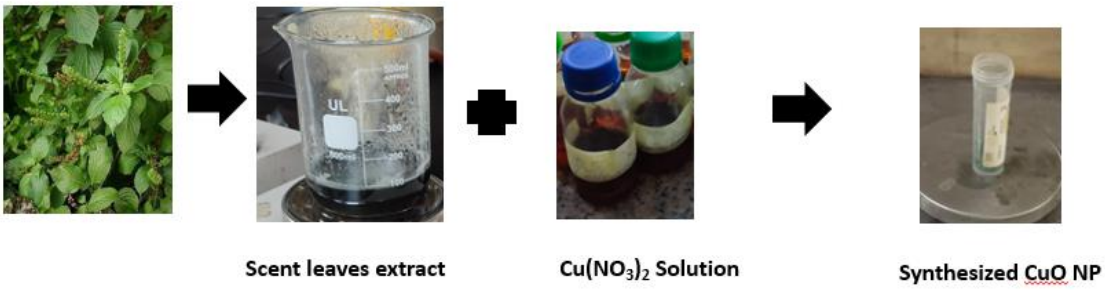


**Plate 2: Synthesis of CuO nanoparticle**

Overall, the reduction can be represented as:
$Cu^{2+} + 2e^- \rightarrow Cu^0$

2. Formation of CuO Nanoparticles:
Upon reduction, the Cu (0) nanoparticles immediately oxidize in the presence of oxygen from the air to form CuO nanoparticles:

$Cu^0 + O_2 \rightarrow CuO$

3. Capping and Stabilization:
During and after the formation of CuO nanoparticles, the phytochemicals in the scent leaf extract act as capping agents, adsorbing onto the surface of the nanoparticles. This capping process stabilizes the nanoparticles, prevents their agglomeration, and controls their growth, leading to well-dispersed and stable CuO nanoparticles.
Therefore, the overall reaction involving scent leaf extract and copper nitrate can be summarized as:

$Cu^{2+}(aq) + 2e^- +$ scent leaf extract $\rightarrow$ CuO nanoparticles + by-products

These reactions highlight how the phytochemicals in scent leaf extract facilitate the green synthesis of CuO nanoparticles by acting as both reducing agents for Cu (II) ions and capping agents for the resulting nanoparticles.

**Fabrication of MDSSC**

**Pastes for insulator spacer layer**

$ZrO_2$ paste was printed on the $TiO_2$ layer to cover the porous $TiO_2$ layer. The $ZrO_2$ paste was then annealed at 450 ° C / 30 min to prepare ZrO layer. (All screen-printing steps were carried out with a screen printer equipped with 70 mesh screen). The $ZrO_2$ paste was printed over the etched line of FTO to avoid contacting between the

photoanode and the counter electrode (Kuang *et al*., 2006).

**Counter Electrode Preparation**

For the reference structure, when the substrate cooled, carbon conductive paste (Elcocarb solaronix) was applied as back contact by doctor blading, which was followed by annealing at 400° C for 30 minutes and printed on the $ZrO_2$ layer. At the same time, the carbon layer was connected to the other FTO layer. However, for the improved counter electrode, when the substrate cooled, carbon conductive paste (Elcocarb solaronix) was applied alongside the carbon nanoparticles as back contact by doctor blading, which was followed by annealing at 400° C for 30 minutes and was printed on the $ZrO_2$ layer (Kuang *et al*., 2006). The porous carbon matrix, which serves as the substrate for the CuO nanoparticles, is prepared separately. This matrix is usually formed by pyrolyzing a carbon precursor material under controlled conditions to create a network of pores suitable for accommodating nanoparticles. The approach employed to deposit CuO nanoparticles onto the porous carbon matrix was achieved by doctor blading, thereby allowing the nanoparticles to infiltrate the pores.

**MDSSC Assembling**

FTO glass plates (TEC-15, Nippon Sheet Glass Co., Ltd., Japan) were utilized to fabricate monolithic electrodes. A pre-cleaning substrate was carried out by washing the FTO substrate with propanol and drying it in a spin coater (Labscience model 800) at 3000 RPM. Ti-Nanoxide was applied by screen printing followed by annealing in at $450^0$ C / 30 min to prepare mesoporous $TiO_2$. The mesoporous films are next treated with a 70 mM solution of $TiCl_4$ at 70° C / 30 min, rinsed with water and annealed at 500° C / 30 min. ZrO2 paste was printed on the TiO2 layer when the substrate was cooled to cover the porous $TiO_2$ layer. The $ZrO_2$ paste was then annealed at $450^0$ C / 30 min to prepare the ZrO layer. (All screen-printing steps were carried out with a screen printer equipped with a 70-mesh screen). The $ZrO_2$ paste was prepared according to a published procedure using $ZrO_2$ nanoparticles (d=40–50nm; Fulka, USA) (Ito *et al*., 2006)**.** When the substrate cooled, carbon conductive paste (Elcocarb solaronix) was applied as back contact by doctor blading, which was followed by annealing at 400° C for 30 minutes and printed on the $ZrO_2$ layer. At the same time, the carbon layer was connected to the other FTO layer. The cell stack is soaked overnight in a dye solution composed of Chlorin e6 dissolved in Toluene and kept at room temperature (Kuang *et al*., 2006). The dye-adsorbed photoanode was withdrawn from the solution, rinsed with toluene, and dried on a hot plate at 60°C in the Dark. The dye-coated electrodes were combined with glass plates by heating a hot-melt glue film at 250°C for 1min (150µm thick; Bynel 4164, DuPont, USA). While still on the hot plate, the temperature is raised to 80°C. Subsequently, a drop of the electrolyte solution 0.05 M solution of CuI dissolved in acetonitrile was applied by drop casting into a hole drilled into the glass of the assembled cell to form the completed cell. Finally, the hole was sealed using aluminium foil (0.1mm thick). The electrolyte was also obtained from solaronix, which has been used in highly durability DSSCs (Kuang *et al*., 2006).

**Characterization Techniques**

The nanoparticles' UV-visible absorption spectra were determined using a Spectrumlab 752 single-beam UV-vis spectrometer, which operates in the 200–800 nm range at room temperature. Spectroscopy using FT-IR Agilent Technologies Cary 630 FT-IR was used to study the nanoparticles and determine functional groups and component combinations. X-ray diffraction (XRD) Analysis for Crystallographic Structure Determination. The current-voltage characteristics have been done to analyse the photovoltaic properties of the cells using a solar simulator (Newport Oriel, instrument model 65194A - 100 solar simulator) at $100mW/cm^2$ coupled with a source measure unit Kethley Model 2400 source meter as shown

**Results and Discussion**

**Optical Absorbance of the Synthesized CuO Nanoparticle**

Fig. 1 displays the CuO nanoparticle's UV–Vis optical absorptions that were synthesized using a fixed ratio of 1:10 of scent leaf and the precursor

and sample collection at different temperatures, ranging from 60 ºC to 100 ºC. Colour change in the precursor solution confirmed the formation of the nanoparticle (Rajesh *et al*., 2017). As the leaf extract and the Copper solution were mixed, the blue colour solution changes to pale bluish green colour due to the formation of CuNPs. The blue colour became intense as the volume of the extract increased. The resulting pale blue-coloured solutions confirmed the synthesis of CuO nanoparticles (Rajesh *et al*., 2017). The optical absorptions observed between 290 nm and around 310 nm belong to CuO nanoparticles, as reported in the literature (Behera *et al.*, 2012; Balamurughan *et al.*, 2014; Yardily *et al.,* 2019). The absorbance peaks increased gradually as the temperature of the extract increased up to 100 ºC. However, the absorbance peak was observed when the extract's temperature was increased to about 100 ºC. As a result, the nanoparticle was successfully synthesized using. To optimize the concentration required to be incorporated into the DSSC photoanode to fabricate the solar cells, the nanoparticle synthesized with 53.33 g of the precursor at about 100 ºC was later used for the fabrication of Counter electrodes for the MDSSC (Salih *et al.*, 2021

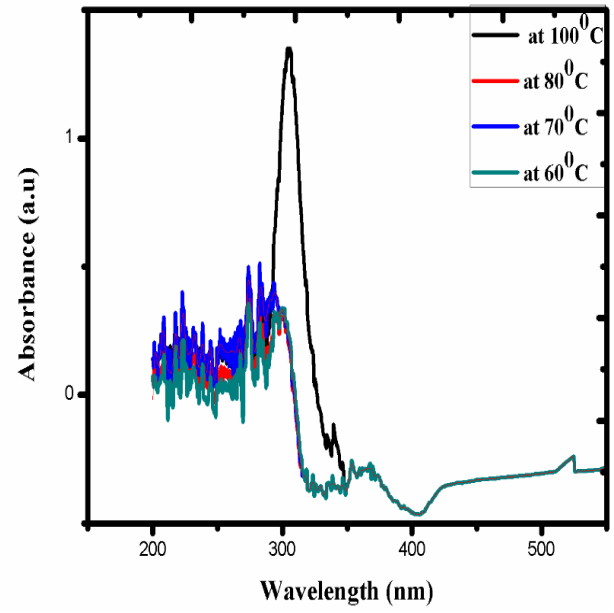


**Fig 1:** Optical absorbance of the synthesized nanoparticle.

## FTIR Spectroscopy

Fig 2 shows the FTIR of the product (Copper oxide Nanoparticles), which displayed a wide stretch of the O-H group at 3372 $cm^{-1}$, C=C at 1624 $cm^{-1}$, C-H at 2279 $cm^{-1}$, N-H at 1640, H-C-H at 2923 and C-O-C at 1197 $cm^{-1}$. The oxidized polyphenols on the synthesized copper oxide Nanoparticles were examined and the ethers or esters, primary amines, asymmetric and symmetric stretch alkanes, alcohols, and phenols could be seen from the various peaks. It may be assumed that the polyphenols in the scent leaf extract may function as a reducing agent as well as a capping agent which are phytochemicals of plant extract responsible for nanoparticle synthesis.

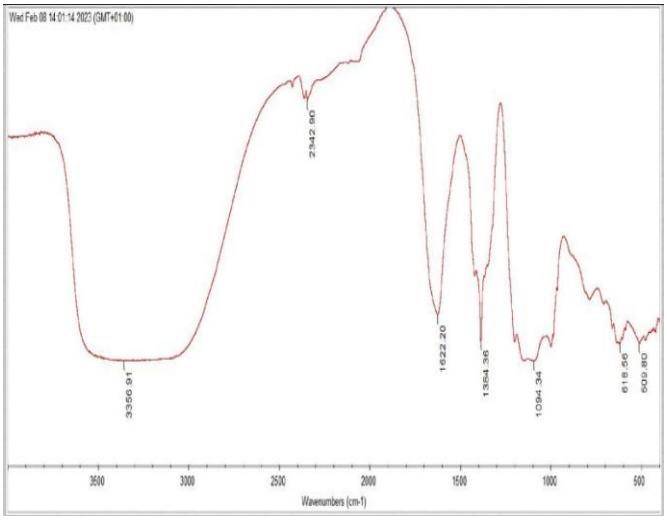


**Fig 2:** FTIR spectra of the synthesized CuO nanoparticle

## Structural studies

The metrics used to assess the crystallinity or amphoric nature of any substance are the sharpness and intensity of the peaks. From Figure 3, CuO makes up the majority of the CuO nanoparticle, as demonstrated by multiple peaks at 2θ around 17.83°, 22.19°, 29.26°, 35.82°, 37.20°, and 39.27°, which are indexed as 111, 210, 220, 222, 320, and 321 planes, respectively. This finding was in good accord with previous investigation studies (Abdulah *et al.*, 2022; Qureshi *et al.*, 2020; Kamil *et al.*, 2021). However, several others indexes present are owned to the glass substrate and the FTO peaks. The CuO belongs to the space group of Cccm and has an orthorhombic shape. The

Debye Scherrer equation, $D = K\lambda / \beta\, Cos\theta$, is used to calculate the crystalline size of the nanoparticles, where D is the nanoparticles crystalline size, K represents the Scherrer constant (0.98), λ denotes the wavelength (1.54), β denotes the full width at half maximum (FWHM) = 0.187. The crystalline size of the nanoparticles was evaluated using a high intense Braggs peak using 2θ = 21.398°, the crystallite size of 45.2nm was evaluated.

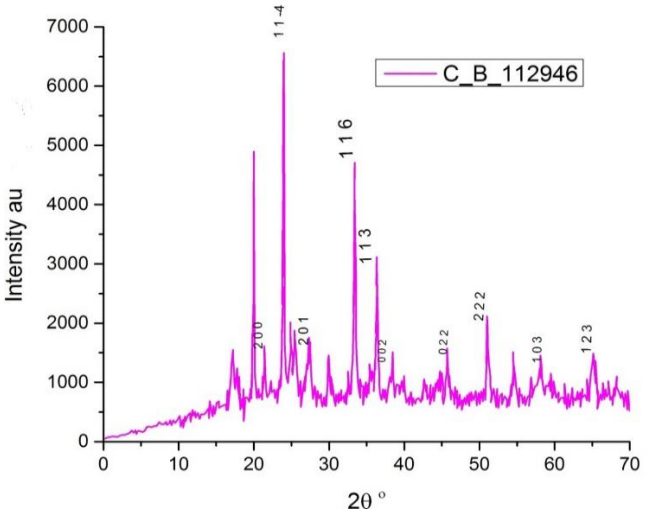


**Fig 3:** XRD pattern of CuO NPs.

**Photovoltaic performance**

The photoanode is fabricated on glass/FTO, and the cathode consists of porous carbon and copper nanoparticles. The anode and cathode are separated using a spacer layer. It is important for the spacer layer to be an insulator with the least current leakage, highly stable in the electrolyte, and possessing sufficient mechanical strength to tolerate pressing pressure. It should also have sufficient porosity to allow ion diffusion. In addition to the porosity produced by removing ethyl cellulose after sintering the layers, the steric hindrance of the particles in the photoanode layer helps decrease the diffusion resistance of ions in the electrolyte. $Al_2O_3$, $TiO_2$ and $SiO_2$ are wide-band gap materials with high chemical stability in the corrosive electrolyte of DSC. In this work, the ZrO2 was utilized as the spacer layer for this monolithic metal-based structure. Photovoltaic characteristics of these devices are reported in Fig 4. and Table 1, respectively. Photovoltaic conversion efficiency and fill factor of solar cells are indicated as PCE and FF, respectively. The device performance of the cells strongly depends on the type of spacer layer. The current density and fill factor are especially affected by the spacer layer.

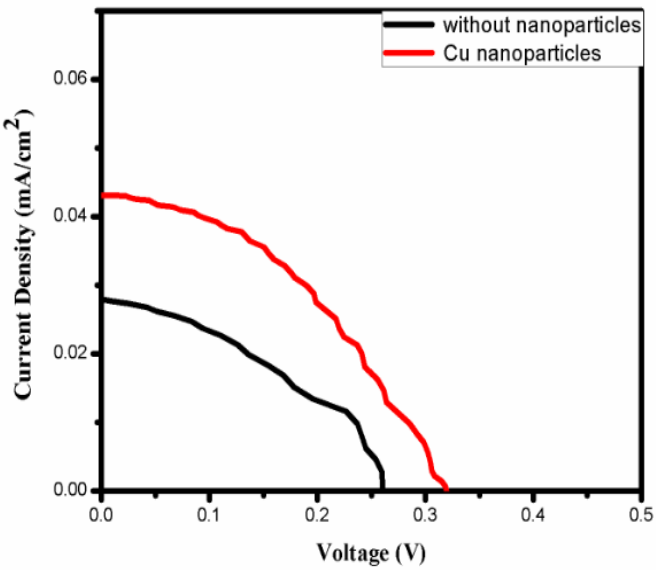


**Fig 4: Current Density versus Voltage curves for Monolithic DSSCs**

The synthesized CuO nanoparticles have been screen-printed onto the FTO to assess how well they work as CEs in DSSCs. By measuring the cell's maximum voltage, maximum current, fill factor, open-circuit voltage and short-circuit current, the performance of the DSSC was assessed. Table 1 presents the performance characteristics of monolithic Dye-Sensitized Solar Cells (DSSCs) with different nanoparticle compositions; without nanoparticles, CuO (Copper oxide) nanoparticles. The parameters measured include open-circuit voltage (Voc), short-circuit current density (Jsc), voltage at maximum power (Vmp), current at maximum power (Imp), fill factor, and overall efficiency. According to Table 1, the solar-to-electric power conversion efficiency of the DSSC made without nanoparticles had the lowest efficiency with 1.7%, an open circuit voltage of 0.2625 V, a short-circuit current of 0.0723 mA/cm$^2$, and a fill factor of 0.3630. The solar-to-electric power conversion efficiency of the CuO CEs was 3.5%, with an open-circuit voltage of 0.3197 V, a short-circuit current of 0.1082 mA/cm$^2$, and a fill factor of 0.41. This shows that the

Table 1: Photovoltaic conversion efficiency of dye-sensitized solar cells (DSSCs) made using nanoparticles of CuO

| Nanoparticles | Voc (V) | Jsc ($mA/cm^2$) | Vmp (V) | Imp ($mA/cm^2$) | Fill factor | Efficiency (%) |
|---|---|---|---|---|---|---|
| Without N.P | 0.2650 | 0.0723 | 0.1359 | 0.0508 | 0.36 | 1.7 |
| CuO | 0.3197 | 0.1083 | 0.1893 | 0.0750 | 0.41 | 3.5 |

introduction of nanoparticles led to a notable increase in Voc compared to the cell without nanoparticles. This suggests that the presence of these nanoparticles influences the voltage characteristics of the monolithic DSSCs. However, the Jsc values of 0.0723 $mA/cm^2$ to 0.123 $mA/cm^2$ indicate the current output when the DSSC is short-circuited. Notably, CuO shows higher Jsc values compared to the cell without nanoparticles, suggesting enhanced light absorption and electron generation in the presence of copper oxide nanoparticles exhibiting higher Vmp and Imp values, indicating an improvement in power conversion efficiency. This suggests that the counter electrode with CuO nanoparticle is particularly effective in facilitating the transfer and utilization of generated electrical energy. The fill-factor efficiency dropped from 0.46 to 0.36. The fill factor is a measure of how well a solar cell can utilize the generated power. In this case, the percentage increase of the cells shows that CuO nanoparticles have a percentage increase of 105.9 % over the cell without nanoparticles. The overall efficiency of the DSSCs is significantly improved with the incorporation of CuO nanoparticles, demonstrating the highest efficiency among the tested compositions, indicating the synergistic effects of combining copper oxide nanoparticles.

The overall improved photovoltaic performance may be attributable to the CuO nanoparticles' surface area, which causes an electron to swiftly move from the CuO NPs to the $TiO_2$. Electrical aspects of light can excite free electrons in metals to create collective oscillations. CuO nanoparticle may experience these oscillations contained in a relatively tiny volume, which enhances the local field and increases light incident on the nanoparticles. As a result, the copper nanoparticles doped with porous carbon increased the light's absorption by the dye-sensitized solar cell, increasing its efficiency. By enhancing the dye absorption of titanium dioxide, the CuO nanoparticles acted as catalysts and since they are good conductors it improved efficiency by raising the short-circuit current density. The open-circuit voltage increased noticeably, and the fill factor also became better.

## Conclusion

It has been demonstrated that a novel green synthesis of CuO nanoparticles can be achieved by using an extract from scent leaves. The absorbance was enhanced by introducing the plants extract into the precursor. FTIR analyses were performed, and the findings indicated the existence of various functional groups and their potential contribution to the nanoparticle’s formation. Additionally, XRD analyses were performed, and the patterns revealed that the synthesized nanoparticle had an average crystallite size of 47.9 nm, indicating that it was crystalline in nature. After the MDSSCs were fabricated, an efficiency of 1.7% was achieved for the cell without the nanoparticles, while efficiency of 3.5% was obtained for the device prepared by this enhanced counter electrode layer with the titanium electrode as the photoanode, the photo-electrochemical performances using CuO nanoparticles enhanced the efficiency by 105.9%; therefore a monolithic DSSC with an enhanced counter electrode is introduced with the advantage of low cost and higher efficiency in comparison with the conventional DSSC structure**.** Introducing CuO nanoparticles into carbon as a counter electrode enhances solar cell performance by

improving electrical conductivity, catalyzing electrochemical reactions, increasing surface area for reaction sites, ensuring stability and durability, and leveraging synergistic effects between CuO nanoparticles and carbon materials. These enhancements collectively contribute to boosting the efficiency and reliability of dye-sensitized solar cells, making them more competitive and suitable for practical applications in renewable energy technologies.

**Declaration of Competing Interest**

The authors declare that none of the work reported in this study could have been influenced by any known competing financial interests or personal relationships.

**Data availability**

Data will be made available on request.

**Acknowledgment**

The authors acknowledge with gratefulness the Pharmaceutical Laboratory, University of Ibadan for the optical characterizations, FTIR characterizations in Bowen University Iwo Osun, Namiroth Nigeria Limited Abuja for the IV characterizations, University Teknologi PETRONAS, Malaysia also for XRD and FE-SEM analysis, and members of Nanotechnology Research Group, LAUTECH, Ogbomoso, for their fruitful discussions and technical input.

**References**

Abdulah, H. I., Rheima, A. M., Hussain, D. H. & Abed, H. J. (2022). Synthesis of $Fe_2O_3$ Nanoparticles by Photolysis Method for Novel Dye-sensitized Solar Cell. *Journal of Advanced Sciences and Nanotechnology*, *1*(1), 1–8.

Adachi, T. & Hoshi, H. (2013) Preparation and characterization of Pt/carbon counter electrodes for dye-sensitized solar cells*, Mater. Lett.* 94, 15–18, http://dx.doi.org/10.1016/j.matlet.2012.11.123.

Adedokun, O., Awodele, M.K., Sanusi, Y.K. & Awodugba, A.O. (2018). Natural dye extracts from fruit peels as sensitizers in ZNO-based dye-sensitized solar cells, *IOP Conf. Ser*. 173, 012040, https://doi.org/10.1088/1755-1315/173/1/012040.

Aghazada, S., Gao, P., Yella, A., Marotta, G., Moehl, T., Teuscher, J., Moser, J.E., De Angelis, F., Grätzel, M. & Nazeeruddin, M.K. (2016). Ligand engineering for the efficient dye-sensitised solar cells with ruthenium sensitizers and cobalt electrolytes*, Inorg. Chem*. 55 (2016) 6653–6659, http://dx.doi.org/10.1021/acs.inorgchem.6b00842.

Ahmad, I., McCarthy, J.E., Bari, M. & Gun'ko, Y. K. (2014). Carbon nanomaterial-based counter electrodes for dye sensitized solar cells*, Sol. Energy 102*, 152–161, http://dx.doi.org/10.1016/j.solener.2014.01.012.

Ahn, H.J., Kim, I.H., Yoon, J.C., Kim, S.I. & Jang, J. H. (2014). p-Doped three-dimensional graphene nano-networks superior to platinum as a counter electrode for dye-sensitized solar cells, *Chem. Commun*. 50, 2412–2415, http://dx.doi.org/10. 1039/c3cc48920e.

Aitken, R.J., Chaudhry, M.O., Boxalland, A.B. & Hull, M. (2006). Manufacture and use of nanomaterials: current status in the UK and global trends, *Occup. Med*. 56 (5), 300–306, https://doi.org/10.1093/occmed/kql051

Anta, J.A., Guillén, E. & Tena-Zaera, R. (2012). ZnO-based dye-sensitized solar cells*, J. Phys. Chem. C* 116, 11413–11425, http://dx.doi.org/10.1021/jp3010025

Bai, Y., Yu, Q., Cai, N., Wang, Y., Zhang, M. & Wang, P. (2011). High-efficiency organic dyesensitized mesoscopic solar cells with a copper redox shuttle*, Chem. Commun*. 47, 4376, http://dx.doi.org/10.1039/c1cc10454c

Baker, J., Deganello, D., Gethin, D. T. & Watson, T .M. (2014). Flexographic printing of graphene nanoplatelet ink to replace platinum as counter electrode catalyst in flexible dye sensitised solar cell, *Mater. Res. Innov* 18, 86–90, http://dx.doi.org/10. 1179/1433075x14y.0000000203.

Balamurughan, M.G., Mohanraj, S., Kodhaiyolii, S., Pugalenthi, V. & Chem, J. (2014*). Pharm. Sci.* 4 201–204, https://doi.org/10.1515/gps-2017-0145.

Behera, S.S., Patra, J.K., Pramanik, K., Panda, N.

& Thatoi, H. (2012). Characterization and evaluation of antibacterial activities of chemically synthesized iron oxide nanoparticles, *World J. Nano Sci. Eng*. 2 196, https://doi.org/10.4236/ wjnse.2012.24026.

Bella, F., Gerbaldi, C., Barolo, C. & Grätzel, M. (2015). Aqueous dye-sensitized solar cells, *Chem. Soc. Rev*. 44, 3431–3473, http://dx.doi.org/10.1039/C4CS00456FHigashino, T. & Imahori, H. (2015). Porphyrins as excellent dyes for dye-sensitized solar cells: recent developments and insights, *Dalt. Trans.* 44, 448–463, http://dx.doi.org/10.1039/c4dt02756f.

Bibi, I., Nazar, N., Ata, S., Sultan, M., Ali, A., Abbas, A., Jilani, K., Kamal, S., Sarim, F.M., Khan, M.I., Jalal, F. & Iqbal, M. (2019) Green synthesis of iron oxide nanoparticles using pomegranate seeds extract and photocatalytic activity evaluation for the degradation of textile dye*, J. Mater. Res. Technol*. 8, 6115–6124, https://doi.org/10.1016/j.jmrt.2019.10.006

Chen, T.Y., Huang, Y.J., Li, C.T., Kung, C.W., Vittal, R. & Ho, K.C. (2017). Metal-organic framework/sulfonated polythiophene on carbon cloth as a flexible counter electrode for dye-sensitized solar cells, *Nano Energy* 32, 19–27, http://dx.doi.org/10.1016/j.nanoen.2016.12.019.

Freitag, M., Teuscher, J., Saygili, Y., Zhang, X., Giordano, F., Liska, P., Hua, J., Zakeeruddin, S.M., Moser, J., Grätzel, M. & Hagfeldt, A., (2017). Dye-sensitized solar cells for efficient power generation under ambient lighting, *Nat. Photon*. 11, 372–378, http://dx.doi.org/10.1038/nphoton.2017.60

Fu, D., Lay, P. & Bach, U. (2013) TCO-free flexible monolithic back-contact dye-sensitized solar cells, *Energy Environ. Sci.* 6, 824, http://dx.doi.org/10.1039/ c3ee24338a.

Fu, D., Li Zhang, X., Barber, R.L. & Bach, U. (2010) Dye-sensitized back-contact solar cells, *Adv. Mater.* 22, 4270–4274, http://dx.doi.org/10.1002/adma.201001006

Gong, J., Sumathy, K., Qiao, Q. & Zhou, Z. (2017). Review on dye-sensitized solar cells (DSSCs): advanced techniques and research trends*, Renew. Sustain. Energy Rev*. 68, 234–246,

Gratzel, M. (2005). Solar energy conversion by dye-sensitized photovoltaic cells, *Inorg. Chem*. 44, 6841–6851, https://doi.org/10.1021/ic0508371.

Huang, Z., Meier, H., & Cao, D. (2016). Phenothiazine-based dyes for efficient dye-sensitized solar cells*, J. Mater. Chem*. C 4, 2404–2426, http://dx.doi.org/10.1039/ C5TC04418A.

Ito, S., Murakami, T.N., Comte, P., Liska, P., Gratzel, C., Nazeeruddin, M.K. & Gratzel, M. (2008) Fabrication of thin film dye sensitized solar cells with solar to electric power conversion efficiency over 10%, Thin Solid Films 516 (14) 4613–4619, https://doi.org/10.1016/j.tsf.2007.05.090

Ito, S. & Takahashi, K. (2012). Fabrication of monolithic dye-sensitized solar cell using ionic liquid electrolyte*, Int. J. Photoenergy* 2012, 1–6, http://dx.doi.org/10.1155/ 2012/915352. .

Kamil, A. F., Abdullah, H. I., Rheima, A. M., Mohammed, S. H., Tumaa, S. J. & Abed, R. M. (2021). Fabrication of $Fe_2CuO_4$ nanoparticles via photolysis technique for improved performance in dye-sensitized solar cells. *Digest Journal of Nanomaterials and Biostructures*, *16*(4), 1453–1460.

Kuang, D., Seigo, I., Bernard, W., Cedric, K., Jacques-E, M., Robin, H., Shaik, Z. & Michael, G. (2006). High molar extinction coefficient heteroleptic ruthenium complexes for thin film dye sensitized solar cells. *Journal of the American chemical society*, 12, 4146-4157.

Kwon, J., Park, N.G., Lee, J.Y., Ko, M.J. & Park, J. H. (2013) Highly efficient monolithic dyesensitized solar cells, *ACS Appl. Mater. Interfaces* 5 2070–2074, http://dx.doi.org/10.1021/am302974z..

Li, T.Y., Su, C., Akula, S.B., Sun, W.G., Chien, H.M. & Li, W.R. (2016). New pyridinium ylide dyes for dye sensitized solar cell applications, *Org. Lett.* 18, 3386–3389, http://dx.doi.org/10.1021/acs.orglett.6b01539.

Liang, M. & Chen, J. (2013). Arylamine organic

dyes for dye-sensitized solar cells, *Chem. Soc. Rev.* 42, 3453, http://dx.doi.org/10.1039/c3cs35372a.

Lin, C.J., Yu, W.Y. & Chien, S.H. (2008). Rough conical-shaped $TiO_2$-nanotube arrays for flexible backilluminated dye-sensitized solar cells, *Appl. Phys. Lett*. 93, 133107, http://dx.doi.org/10.1063/1.2992585

Lin, C.Y., Lai, Y.H., Chen, H.W., Chen, J.G., Kung, C.W., Vittal, R. & Ho, K.C. (2011). Highly efficient dye-sensitized solar cell with a ZnO nanosheet-based photoanode, *Energy Environ. Sci.* 4, 3448, http://dx.doi.org/10.1039/c0ee00587h. 013-0346-6.

Liu, G., Wang, H., Li, X., Rong, Y., Ku, Z., Xu, M., Liu, L., Hu, M., Yang, Y., Xiang, P., Shu, T. & Han, H. (2012). A mesoscopic platinized graphite/carbon black counter electrode for a highly efficient monolithic dye-sensitized solar cell, *Electrochim. Acta* 69, 334–339, http://dx.doi.org/10.1016/j.electacta.2012.03.012.

Lizama-Tzec, F.I., Garcia-Rodriguez, R., Rodriguez-Gattorno, G., Canto-Aguilar, E.J., Vega-Poot, A.G., Heredia-Cervera, B.E., Villanueva-Cab, J., Morales-Flores, N., Pal, U. & Oskam, G. (2018). Influence of morphology on the performance of ZnO-based dye-sensitized solar cells, *RSC Adv.* 6 (2016) 37424–37433, http://dx.doi.org/10.1039/

Oskam, G., Bergeron, B.V., Meyer, G.J. & Searson, P. C. (2001). Pseudohalogens for dye-sensitized TiO, {2} photoelectrochemical cells, *J. Phys. Chem*. B 105, 6867–6873, http://dx.doi.org/10.1021/jp004411d.

Pettersson, H., Gruszecki, T., Johansson, L.H. & Johander, P. (2003). Manufacturing method for monolithic dye-sensitised solar cells permitting long-term stable low-power modules, *Sol. Energy Mater. Sol. Cells* 77, 405–413, http://dx.doi.org/10.1016/ S0927-0248(02)00368-9.

Qureshi, A. A., Javed, S., Asif Javed, H. M., Akram, A., Jamshaid, M. & Shaheen, A. (2020). Strategic design of Cu/$TiO_2$-based photoanode and rGO-$Fe_3O_4$-based counter electrode for optimized plasmonic dye-sensitized solar cells. *Optical Materials*, *109*.

Rajesh, K.M., Ajitha, B., Ashok Kumar Reddy, Y., Suneetha, Y. and Sreedhara Reddy P. (2017) Assisted green synthesis of copper nanoparticles using Syzygium aromaticum bud extract: Physical, optical, and antimicrobial properties, *Optik.* 154, 593 – 600, https://doi.org/10.1016/j.ijleo.2017.10.074

Rong, Y., Liu, G., Wang, H., Li, X. & Han, H. (2013). Monolithic all-solid-state dye-sensitized solar cells, *Front. Optoelectron*. 6, 359–372, http://dx.doi.org/10.1007/ s12200-

Roy, P., Kim, D., Lee, K., Spiecker, E. & Schmuki, P. (2010). $TiO_2$ nanotubes and their application in dye-sensitized solar cells, *Nanoscale* 2, 45–59, http://dx.doi.org/ 10.1039/b9nr00131j.

Salih, W. M., Rheima, A. M. & Kadhum, H. A. (2021). Synthesis and Characterization of CeO (x-) CuO (1-x Nanocomposite by Simple Aqueous Route for Solar Cell Application.

Sharmoukh, W. & Allam, N. K. (2012). $TiO_2$ nanotube-based dye-sensitized solar cell using new photosensitizer with enhanced open-circuit voltage and fill factor, *ACS Appl. Mater. Interfaces* 4, 4413–4418, http://dx.doi.org/10.1021/am301089t. .

Takeda, Y., Kato, N. & Toyoda, T. (2009) Advances in monolithic series-interconnected solarcell development, *SPIE Newsroom* 2–4, http://dx.doi.org/10.1117/2. 1200903.1581.

Thompson, S.J., Pringle, J.M., Zhang, X.L. & Cheng, Y.B. (2013) A novel carbon–PEDOT composite counter electrode for monolithic dye-sensitized solar cells, *J. Phys. D Appl. Phys.* 46, 24007, http://dx.doi.org/10.1088/0022-3727/46/2/ 024007

Wang, H., Liu, G., Li, X., Xiang, P., Ku, Z., Rong, Y., Xu, M., Liu, L., Hu, M., Yang, Y. & Han, H. (2011). Highly efficient poly(3-hexylthiophene) based monolithic dye-sensitized solar cells with carbon counter electrode, *Energy Environ. Sci.* 4, 2025–2029, http://dx.doi.org/10.1039/c0ee00821d

Wild, M., Griebel, J., Hajduk, A., Friedrich, D., Stark, A., Abel, B. & Siefermann, K.R. (2016). Efficient synthesis of triarylamine-based dyes

for p-type dye-sensitized solar cells, *Sci. Rep*. 6, 26263, http://dx.doi.org/10.1038/srep26263. http://dx.doi.org/10.1016/j.rser.2016.09.097.

Yardily, A. & Sunitha, N. (2019). Green synthesis of iron nanoparticles using hibiscus leaf extract, characterization, antimicrobial activity, *Int. J. Sci. Res.* Rev. 8 (7), https://doi.org/10.1155/2022/5474645.

Yella, A., Lee, H.W., Tsao, H.N., Yi, C., Chandiran, A. K., Nazeeruddin, M.K., Diau, G., Yeh, C.Y., Zakeeruddin, S.M. & Gratzel, M. (2011). Porphyrin-sensitized solar cells with cobalt (II/III)-Based redox electrolyte exceed 12 percent efficiency*, Science 334*, 629–634, http://dx.doi.org/10.1126/science.1209688. .

Yu, Y., Zheng, H., Zhang, X., Liang, X., Yue, G., Li, F., Zhu, M., Li, T., Tian, J. & Yin, G. (2016). An efficient dye-sensitized solar cell with a promising material of Bi 4 Ti 3 O 12 nanofibers/graphene, *Electrochim. Acta* 215, 543–549, http://dx.doi.org/10. 1016/j.electacta.2016.08.086.

Zebardastan, N., Khanmirzaei, M.H., Ramesh, S. & Ramesh, K. (2017). Performance enhancement of poly (vinylidene fluoride-co-hexafluoro propylene)/polyethylene oxide-based nanocomposite polymer electrolyte with ZnO nanofiller for dye-sensitized solar cell, *Org. Electron*. 49, 292–299, http://dx.doi.org/10.1016/j.orgel. 2017.06.062.

Zhu, S., Shan, L., Tian, X., Zheng, X., Sun, D., Liu, X., Wang, L. & Zhou, Z. (2014). Hydrothermal synthesis of oriented ZnO nanorod-nanosheets hierarchical architecture on zinc foil as flexible photoanodes for dye-sensitized solar cells*, Ceram. Int*. 40, 11663–11670, http://dx.doi.org/10.1016/j.ceramint.2014.03.173.

Zi, M., Zhu, M., Chen, L., Wei, H., Yang, X. & Cao, B. (2014). ZnO photoanodes with different morphologies grown by electrochemical deposition and their dye-sensitized solar cell properties*, Ceram. Int.* 40, 7965–7970, http://dx.doi.org/10.1016/j. ceramint.2013.12.146.

.
.
.